Capabilities and constraints of NorSand in modelling slope instability

P.A. Crous & S.W. Jacobsz

Department of Civil Engineering, University of Pretoria, Pretoria, South Africa

ABSTRACT: Numerical modelling is an essential tool for understanding slope instability, especially when paired with robust constitutive models. This study evaluates the application of the NorSand model in finite element method (FEM) back-analyses to simulate slope failures. NorSand, rooted in critical state soil mechanics, effectively captures soil responses such as dilatancy and contraction, making it suitable for analysing both loose and dense soils. A back-analysis of a centrifuge test on a loose sand slope subjected to a rising water table demonstrated NorSand's ability to predict stress state evolution and drained instability, providing valuable insights into slope stability mechanisms. However, limitations were observed in capturing post-failure behaviour, including large deformations and the pore pressure responses measured during failure. This study highlights NorSand's potential as a predictive tool while cautioning against its use for post-failure analyses. Recommendations are provided for refining its application and integrating it with experimental data to improve slope stability assessments.

1 INTRODUCTION

Understanding slope instability mechanisms is critical for geotechnical engineering, particularly in the design and management of slopes in challenging conditions. Numerical modelling has become an indispensable tool for analysing these mechanisms, providing detailed insights into stress evolution, deformation, and failure processes. Among the many available constitutive models, NorSand – a critical state soil mechanics-based model – has gained prominence for its ability to simulate the complex behaviour of granular soils. The NorSand model is also applicable for capturing the response of non-cohesive fine grained soils. Its strength lies in capturing prefailure mechanisms, such as dilatancy and contraction, which are vital for understanding slope responses under varying conditions.

This study focuses on evaluating the application of the NorSand model within finite element method (FEM) back-analyses, particularly for slopes subjected to drained instability triggers. Through a back-analysis of a centrifuge test on a loose sand slope with a rising water table, the study demonstrates the model's effectiveness in capturing key behavioural trends and instability triggers. However, challenges remain in simulating post-failure behaviour, including large deformations and pore pressure responses, which limit its utility in certain scenarios. This paper

aims to provide a balanced assessment of the capabilities and limitations of NorSand, offering insights for refining its application and improving the reliability of numerical modelling in geotechnical engineering.

2 METHODOLOGY

2.1 Centrifuge test

The centrifuge test was conducted at the University of Pretoria. More details about the geotechnical centrifuge are provided by Jacobsz et al. (2014). The general centrifuge package was similar to that presented by Crous et al. (2022) and Ng et al. (2023). The model slope was constructed from a commercially available fine silica sand obtained from a quarry near Cullinan, South Africa. The slope was constructed using moist tamping (void ratio of 0.9), creating a soil fabric susceptible to liquefaction. Figure 1 shows a schematic diagram of the package and model slope, along with the instrumentation installed in the slope. Tensiometers (pore pressure) and linear variable differential transformers (LVDTs; displacement) were installed in the slope. The tensiometers are labelled T1 - T5 in Figure 1. The slope was constructed to an angle of 35°, which was steeper than the friction angle (Φ'_c) of 33°. During the test, the slope settled to an angle of 32°. A reservoir was created at the upstream section of the slope using a geotextile covered perforated

plate. This allowed for control over the hydraulic head at the upstream of the model. The model was accelerated to 30 g. Once at the elevated acceleration, the reservoir was filled with a water-glycerine mixture with a viscosity of $\sqrt{30}$ higher than water (Askarinejad et al. 2015, Crous et al. 2022). The fluid seeped through the slope, raising the water table until drained instability was triggered (i.e. drained factor of safety reduced to below one).

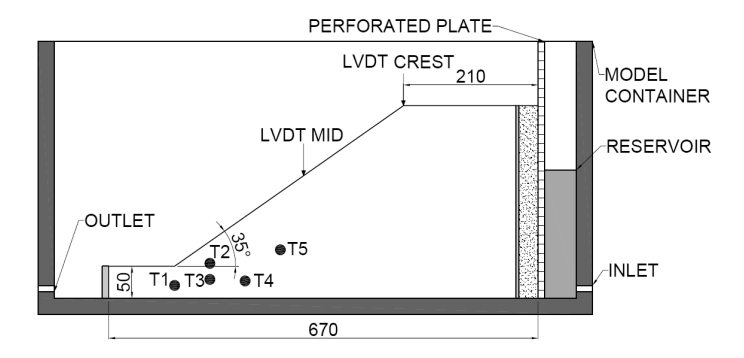


Figure 1. Schematic diagram of centrifuge test.

2.2 NorSand model

The calibration of the NorSand model followed the procedure recommended by Shuttle & Jefferies (2010), with calibrated parameters summarised in Table 1. A series of drained and undrained triaxial tests were conducted on both dense and loose specimens. Figure 2a and b show the measured (solid lines) and NorSand predicted (dashed lines) stress-strain response and effective stress paths of three undrained triaxial compression tests, respectively. All three tests were conducted on loose specimens, meaning the specimens were susceptible to liquefaction. The calibrated model agrees well with the measured responses. The main characteristic of the NorSand model is that it is capable of capturing the instability and liquefaction of the Cullinan sand that was observed in the series of triaxial tests.

Table 2. NorSand parameters.

| 1 | |
|---|--------|
| Parameter | Value |
| Void ratio of CSL at $p' = 1$ kPa; Γ | 0.8698 |
| Slope of CSL in $e - \ln p'$ space; λ | 0.0202 |
| Critical state ratio; M | 1.329 |
| Reference elastic shear modulus; G_{ref} | 20 MPa |
| Elastic exponent; m | 0.5475 |
| Poisson's ratio; v | 0.3 |
| Volumetric coupling coefficient; N | 0.2375 |
| State-dilatancy parameter; χ_{tc} | 3.5 |
| Plastic hardening modulus (base); H_0 | 130.1 |
| Plastic hardening modulus; H_{ν} | 1439 |
| · · · · · · · · · · · · · · · · · · · | |

In addition to the calibrated NorSand model, a calibrated Van Genuchten soil water retention curve (SWRC) was added to the model (Fig. 3). The initial water content was set to 0.1, which corresponded to the initial suction of 15 kPa measured at the start of the centrifuge test.

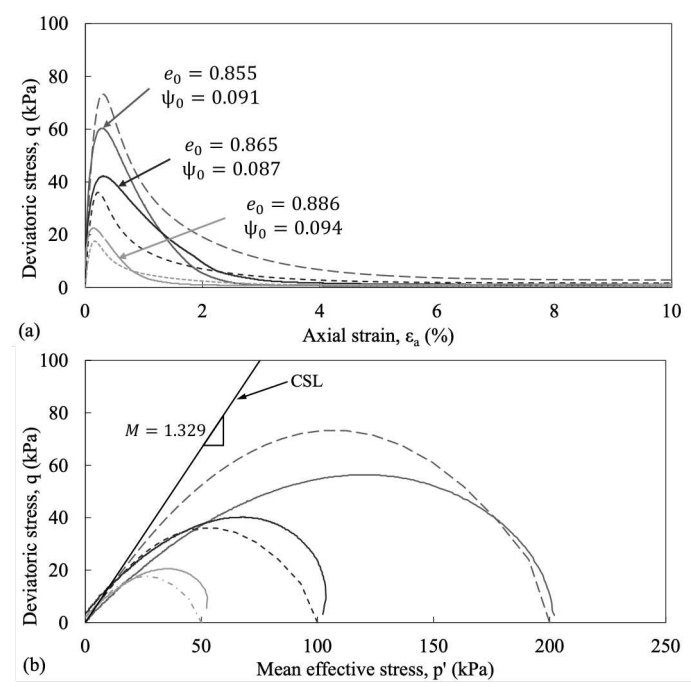


Figure 2. Comparison between measured and NorSand predicted undrained triaxial compression tests: (a) stress-strain responses; and (b) effective stress paths.

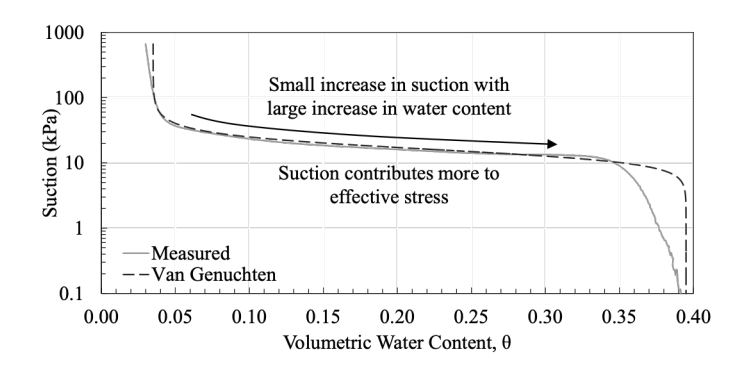


Figure 3. Measured and Van Genuchten predicted SWRC for Cullinan sand.

2.3 Finite element mesh, boundary conditions and modelling procedure

The FEM back-analysis of the centrifuge test was conducted using the commercially available software, PLAXIS 2D. The back-analysis employed the two-dimensional mesh and boundary conditions shown in Figure 4. A fine mesh with 15-node elements was adopted and the analysis was conducted at prototype scale to simplify the modelling. Boundary conditions were set to align with the centrifuge setup: the left and right boundaries were defined with roller connections, while the base boundary was fully fixed. The slope face and toe were set as seepage boundaries, with the bottom and downstream boundaries defined as impervious. A state parameter of 0.03 was applied to the model, in line with the state of the soil where the slip failure occurred.

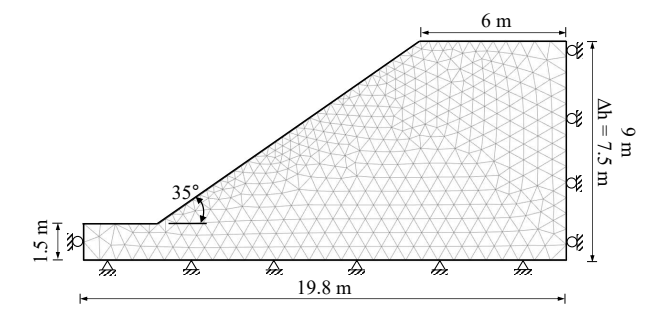


Figure 4. Finite element mesh, dimensions and boundary conditions for numerical back-analysis of centrifuge test.

The modelling process involved three stages. In the first stage, initial conditions were established using gravity loading using a Mohr-Coulomb model, with a Φ'_c of 33° and cohesion of 1 kPa. In the second stage, the constitutive model was switched to NorSand. In the third stage, a 7.5 m hydraulic head was applied to the upstream boundary within a fully coupled flow-deformation analysis, corresponding to the head applied in the centrifuge test. Here, the water table progressively rose until drained instability was induced. Throughout the analysis, stress points corresponding to the tensiometer locations (Fig. 1) were monitored, facilitating direct comparison between measured and simulated responses.

3 SLOPE FAILURE IN CENTRIFUGE TEST

Figure 5a shows the side profile of the slope in the centrifuge test immediately before any visual movement was detected. As soon as the water table had saturated the toe of the slope, drained instability was triggered. The slip surface extended from the toe towards the crest (Fig. 5b). The entire failure event was rapid, with it lasting less than 0.3 seconds.

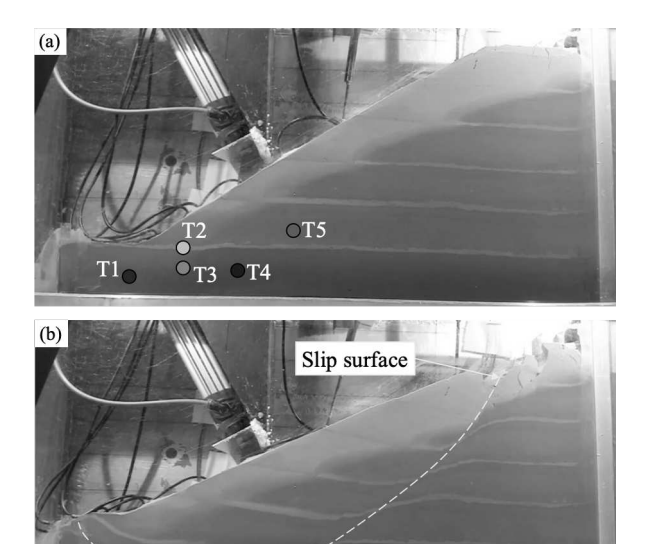


Figure 5. Side profile of failure mechanism in centrifuge test at (a) 0 seconds; (b) 0.3 seconds.

Figure 6a and b illustrate the settlement and excess pore pressures measured immediately before and during the failure of the slope. The vertical dashed line marked "a" corresponds to the time at which Figure 5a was captured. Roughly 5 seconds prior to the slip failure, the slope's settlement began to accelerate gradually (Fig. 6a). This movement indicates that initial shearing was occurring within the soil.

At this early stage, no excess pore pressures were detected (Fig. 6b). A slight increase in pore pressures between 1.2 to 2.0 kPa was measured by tensiometers T2 and T4, following the onset of shearing. The accelerating shearing caused excess pore pressures to develop. However, the initial movement within the slope occurred before these excess pore pressures were measured, indicating that the failure initiated as drained instability. Thus, the failure was a drained to undrained transitional failure.

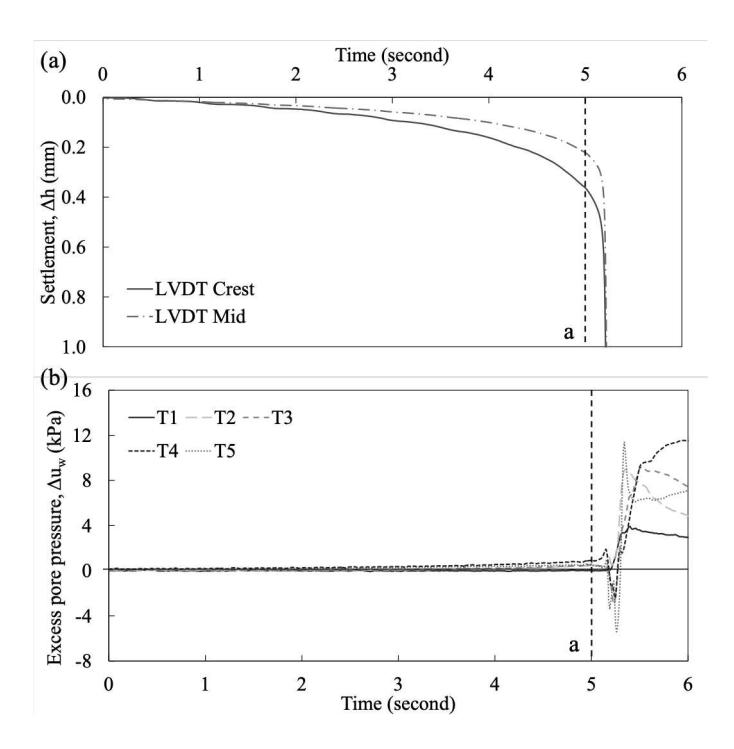


Figure 6. (a) Settlement; (b) excess pore pressures measured during the failure in the centrifuge test.

After failure initiation, the tensiometers recorded a slight reduction in excess pore pressures, followed by a subsequent increase, with peak excess pore pressures of 11.4 kPa. This contractive tendency of the soil contributed to a marked reduction in shear strength once failure was triggered, intensifying the overall failure. Greater reductions in shear strength typically correspond to increased travel distances of the failed soil mass.

4 BACK-ANALYSIS OF CENTRIFUGE TEST

Figure 7 presents the computed effective stress paths of all the monitored stress points, beginning from anisotropic conditions without significant changes following gravity loading and the switch to the NorSand model. Initially, the mean effective stress (p') increased with little changes in deviatoric stress. This increased p' resulted from Bishop's (1959) effective stress:

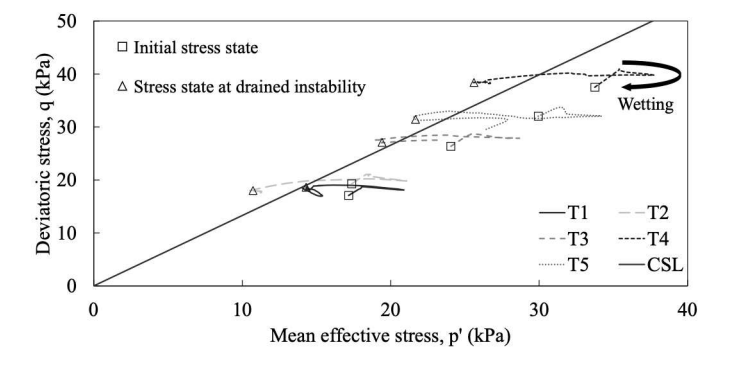


Figure 7. Effective stress paths of the monitored stress points during the back-analysis of the centrifuge test.

$$\sigma' = \sigma + S_{eff} \times h \tag{1}$$

where σ' is effective stress; σ is total stress; S_{eff} is related to the degree of saturation and h is matric suction. The initial water content, around 0.1, meant that 10% of the suction contributed to the soil's effective stress (Fig. 3). As the degree of saturation increased with the rising water table, suction's contribution to effective stress also increased. When the soil became saturated and pore pressures turned positive, effective stress began to decrease, following a constant shear drained (CSD) stress path due to the rising water table (Ng et al. 2023).

Drained instability, marked by the triangular markers, initiated a slight decrease in mean effective stress, trending towards the critical state line (CSL). During the failure, pore pressure fluctuations were computed, after which the analysis reached non-convergence, which indicates runaway plastic strains, and denotes slope failure (Griffiths & Lane 1999).

The stress states were slightly past the CSL at the time of instability. Ng et al. (2023) also observed this and noted that it was due to the lack of an internal cap in the current implementation of NorSand in PLAXIS 2D, which limits the hardening of the yield surface when implemented (Jefferies, 1997). However, Ng et al. (2023) also noted that despite the lack of the internal cap, the NorSand model can still model the onset of drained instability during a CSD stress path, albeit at higher stress ratios.

Figure 8 displays the shear strain distribution at the point of non-convergence, with the phreatic surface in the back-analysis closely matching the observed

surface in Figure 5. In the back-analysis, drained instability initiated at the toe, evident by the concentration of shear strain in that region, and the slip surface propagated towards the crest. The location, size, and depth of the predicted slip surface closely align with the observed failure in Figure 5b. However, the model reached non-convergence well before the failed soil mass was in the location shown in Figure 5b, indicating that NorSand paired with the FEM should not be used for post-failure deformation analyses.

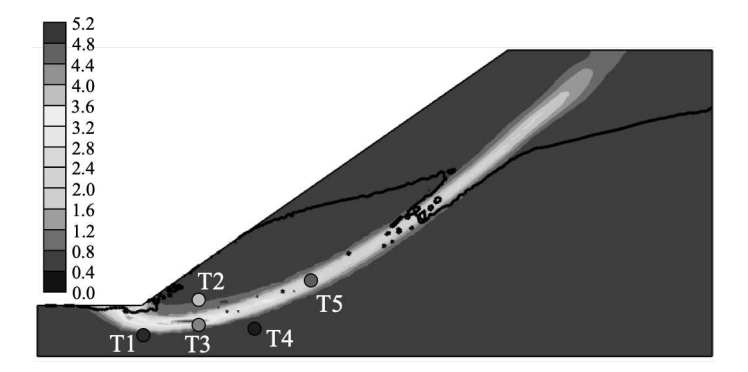


Figure 8. Computed shear strain (%) during FEM back-analysis of centrifuge test.

Figure 9 shows the computed excess pore pressure distribution throughout the failure in the numerical back-analysis, with significant dilation along the slip surface. Figure 10 presents the excess pore pressures for the monitored stress points over time during the failure. The model did not capture the initial contraction seen in the centrifuge test (Fig. 6b). Instead, it immediately predicted strong dilation, with excess pore pressures rapidly becoming negative. However, post-dilation, T1 and T2 showed positive excess pore pressures before non-convergence was reached. It is possible that mesh distortion near these points introduced numerical instability, affecting stress and strain calculations in zones with concentrated shearing. This caused positive excess pore pressure generation as the elements no longer represented the true geometry or physical behaviour of the soil.

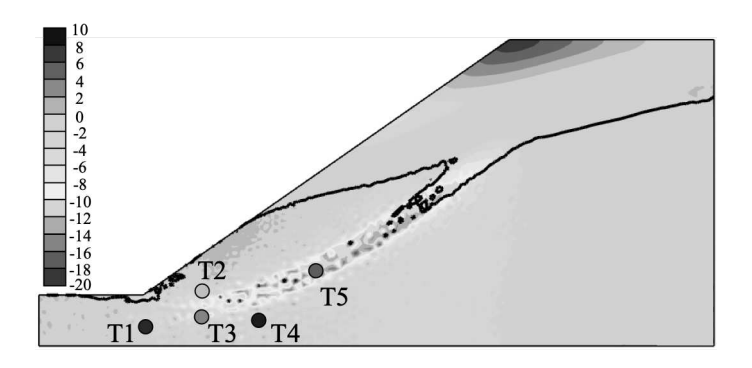


Figure 9. Computed excess pore pressures (kPa) during the failure of the slope in the FEM back-analysis of the centrifuge test.

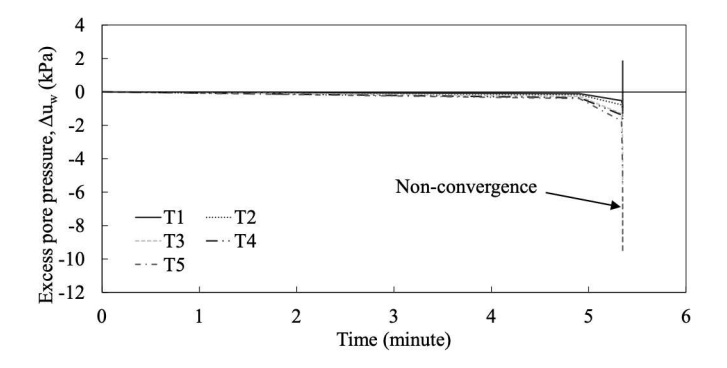


Figure 10. Computed excess pore pressures during failure for the FEM back-analysis of the centrifuge test.

5 CONCLUSIONS

The FEM paired with a complex constitutive model, such as NorSand, has seen widespread adoption by practitioners when investigating slope behaviour. This combination has shown to capture pre-failure mechanisms, such as the development of stress paths, well. Additionally, the model was capable of predicting the onset of drained instability in the loose sand slope relatively well.

Capturing the development of stress states in slopes can help practitioners better understand how close a slope is to instability. This can help with the design of and aid in analysing the stability of the slopes. It can also help practitioners develop and design stabilisation methods and strategies for the slopes.

However, despite the variety of capabilities of the combination of NorSand and the FEM, it is also important to note the constraints of the models. Due to the lack of the internal cap in NorSand in the current implementation in PLAXIS 2D, the onset of instability may be predicted at higher stress ratios than when instability will be triggered in practice.

Additionally, the model could not capture the pore pressure responses measured during the failure of the slope, suggesting that investigating post-failure mechanisms should not be done using this combination.

ACKNOWLEDGMENTS

The authors would like to acknowledge and thank the funding support provided by Anglo American as part of the Anglo American Tailings Study.

REFERENCES

Askarinejad, A., Beck, A. & Springman, S.M. 2015. Scaling law of static liquefaction mechanism in geocentrifuge and corresponding hydromechanical characterization of an unsaturated silty sand having a viscous pore fluid. *Canadian Geotechnical Journal* 52(6): 708-720.

Bishop, A.W. 1959. The principle of effective stress. *Teknisk Ukeblad I Samarbeide Med Teknikk* 106(39): 859-863. Oslo, Norway.

Crous, P.A., Ng, C.W.W. & Jacobsz, S.W. 2022. Lessons learnt modelling tailings dam flow-type failure in the centrifuge. In Proceedings of the 10th International Conference on Physical Modelling in Geotechnics 281-284. London: International Society for Soil Mechanics and Geotechnical Engineering.

Griffiths, D.V. & Lane, P.A. 1999. Slope stability analysis by finite elements. *Géotechnique* 49(3): 387-403.

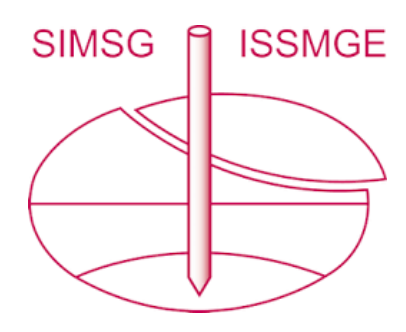
Jacobsz, S.W., Kearsley, E.P. & Kock, J.H.L. 2014. The geotechnical centrifuge facility at the University of Pretoria. 8th International Conference on Physical Modelling in Geotechnics. Perth, Australia.

Jefferies, M.G. 1997. Plastic work and isotropic softening in unloading. *Géotechnique* 47(5): 1037-1042.

Ng, C.W.W., Crous, P.A. & Jacobsz, S.W. 2023. Centrifuge and Numerical Modelling of Liquefied Flow and Nonliquefied Slide Failure of Tailings Dams. *Journal of Geotechnical and Geoenvironmental Engineering* 149(9).

Shuttle, D. & Jefferies, M. 2010. NorSand: Description, calibration, validation and applications.

INTERNATIONAL SOCIETY FOR SOIL MECHANICS AND GEOTECHNICAL ENGINEERING



This paper was downloaded from the Online Library of the International Society for Soil Mechanics and Geotechnical Engineering (ISSMGE). The library is available here:

https://www.issmge.org/publications/online-library

This is an open-access database that archives thousands of papers published under the Auspices of the ISSMGE and maintained by the Innovation and Development Committee of ISSMGE.

The paper was published in the proceedings of the 2nd Southern African Geotechnical Conference (SAGC2025) and was edited by SW Jacobsz. The conference was held from May 28th to May 30th 2025 in Durban, South Africa.